JOC The Journal of Organic Chemistry

Article

pubs.acs.org/joc

Synthesis and Characterization of Thieno[3,4-*b*]pyrazine-Based Terthienyls: Tunable Precursors for Low Band Gap Conjugated Materials

Ryan L. Schwiderski and Seth C. Rasmussen*

Department of Chemistry and Biochemistry, North Dakota State University, NDSU Dept. 2735, P.O. Box 6050, Fargo, North Dakota 58108-6050, United States

Supporting Information

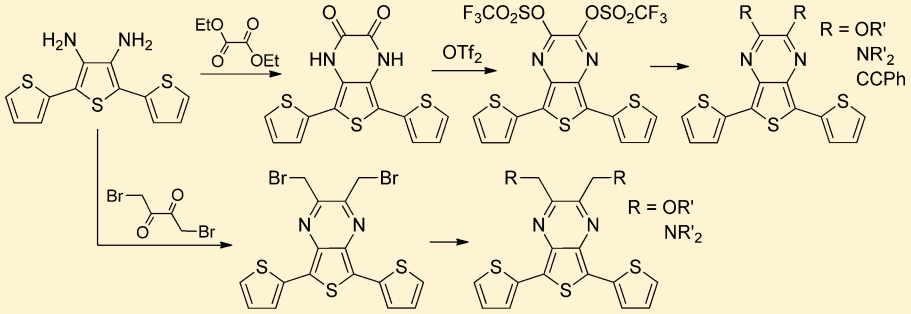

ABSTRACT: Synthetic methods have been developed for the preparation of new 2,3-dihalo- and 2,3-ditriflato-5,7-bis(2-thienyl)thieno[3,4-*b*]pyrazines. From these reactive intermediates, a variety of new 2,3-difunctionalized 5,7-bis(2-thienyl)-thieno[3,4-*b*]pyrazines have been produced as precursors to conjugated materials. Structural, electronic, and optical characterization of these new analogues illustrate the extent to which the electronic nature of the functional groups can be used to tune the electronic properties of these thieno[3,4-*b*]pyrazine-based terthienyl units.

INTRODUCTION

The fused-ring thieno[3,4-*b*]pyrazine (TP) unit[1] has become a quite popular building block and has been shown to be very successful in producing reduced band gap (E_g = 1.5−2.0 eV)[2,3] and low band gap (E_g < 1.5 eV)[2−4] conjugated organic materials. As the material's band gap determines a number of the desirable properties of conjugated polymers, control of this critical parameter is an important factor in the production of technologically useful materials and the application of TPs has been one of the more successful approaches to this goal.[2] Although the simple TP unit has been frequently used as a monomer in the production of numerous homo- and co-polymeric materials,[2−4] some materials scientists find these monomeric units difficult to work with due to their somewhat reactive nature. As a consequence, many favor the application of the terthienyl analogues such as 5,7-bis(2-thienyl)thieno[3,4-*b*]pyrazine[5,6] (Scheme 1, **4a**), in which the reactive α-positions of the TP are substituted with 2-thienyl groups. While these TP-based terthienyls actually undergo oxidation at lower potentials than the simple TP monomers, the increased size and conjugation length of the oligomeric analogues results in slower reactivity and thus a lower chance of loss of product to unwanted oxidative coupling or decomposition.

The first examples of TP-based terthienyls were reported by Yamashita and co-workers in 1994,[5] and these oligomeric species have since become common precursors to TP-based copolymeric materials.[4] Such TP-based terthienyls are prepared in a method analogous to the monomeric TPs as shown in Scheme 1. Here, the bromo functionalities of the common precursor 2,5-dibromo-3,4-dinitrothiophene (**1**)[7] are utilized to generate the 3′,4′-dinitro-2,2′:5′,2″-terthiophene (**2**) via Stille coupling with 2-(tributylstannyl)thiophene. Reduction of **2** to generate the diamine **3** then allows condensation with various

Scheme 1. Synthesis of Simple Thieno[3,4-*b*]pyrazine-Based Terthienyls via Condensation

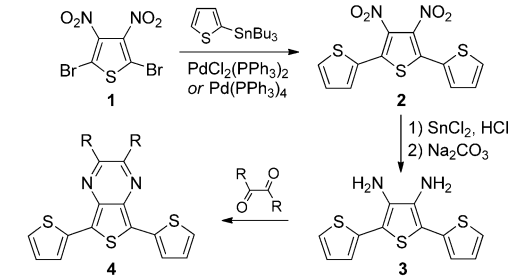

a R = H
b R = CH_3
c R = C_2H_5
d R = C_6H_{13}
e R = $C_{13}H_{27}$
f R = Ph
e R = 4-BrPh
f R = 4-$PhOC_8H_{17}$
g R = 4-(2-ethylhexyloxy)Ph
h R = 4-$PhCO_2R'$
i R = 3-thienyl
j R = 2-pyridyl

Received: March 19, 2013
Published: May 21, 2013

   dx.doi.org/10.1021/jo400577q | *J. Org. Chem.* 2013, 78, 5453−5462

α-diones to generate the central TP unit of the final terthienyl **4**. These methods have since been used to produce a wide variety of unfunctionalized,[5,6] dialkyl,[5,8−13] diaryl,[14−22] and even heteroaryl[16a,17,23−25] TP-based terthienyls.

The choice of functional groups for either the monomeric TPs or the terthienyl analogues here is dependent on the α-dione employed as illustrated in Scheme 1. As a consequence, this has limited the functional groups to either alkyl or aryl, thus resulting in a very narrow range of electronic variance and restricting the extent of possible tuning available in the application of these fused-ring units to the production of low band gap materials. In order to overcome this limitation, our group has recently reported new synthetic methods for the production of monomeric TPs which allows the incorporation of a wide variety of side chains, including both strongly electron-donating and -withdrawing groups.[26] This current report now expands this new synthetic approach to the TP-based terthienyls through the synthesis of new 2,3-difunctionalized 5,7-bis(2-thienyl)thieno[3,4-*b*]pyrazines containing facile leaving groups (Chart 1) as precursors to a variety of new

Chart 1. Thieno[3,4-*b*]pyrazine-Based Terthienyls with Good Leaving Groups

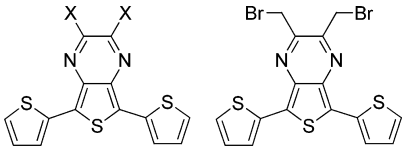

5 X = Br
6 X = OSO_2CF_3
7

analogues. Initial efforts in the application of terthienyl **7** to tunable functionalized TP-based terthienyls have been recently reported as part of a study on side chain tuning of TP-based materials.[27] The synthetic versatility of the precursor species **5**−**7** has been demonstrated here with the production of new TP-terthienyls containing electron-donating and -withdrawing groups. The characterization of these new molecular precursors provide further insight to the extent that the electronic properties of these species can be tuned through varying the respective TP functional groups.

RESULTS AND DISCUSSION

Synthesis. 2,3-Dibromothieno[3,4-*b*]pyrazine (**9**), the monomeric TP analogue of terthienyl **5**, was previously prepared via the intermediate thieno[3,4-*b*]pyrazine-2,3-(1*H*,4*H*)-dione (**8**)[26] as illustrated in Scheme 2. Using this synthetic methodology as a starting point, this same basic approach was then applied to the generation of **5**. However, treatment of the diamine **3** with diethyl oxalate using the previously successful conditions resulted in very low yields (<10%) of the desired product **10**, with the majority of the

Scheme 2. Previous Synthesis of 2,3-Dibromothieno[3,4-*b*]pyrazine

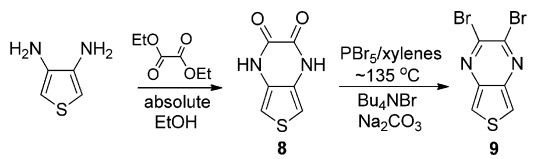

8 **9**

material isolated consisting of the noncyclized product **11** as shown in Scheme 3. The addition of a catalytic amount of HCl resulted in significantly higher yields, but now generated a mixture of **10** and byproduct **12** (Scheme 3).

Scheme 3. Synthesis of 5,7-Bis(2-thienyl)thieno[3,4-*b*]pyrazine-2,3(1*H*,4*H*)-dione

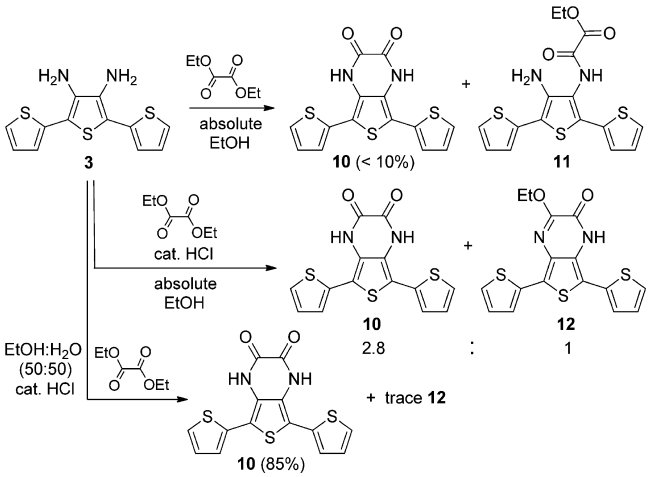

Although **10** could be selectively extracted from the mixture by aqueous KOH, the ratio of the two species in the mixture was approximately 2.8:1, resulting in a significant loss of yield. Attempts to shift this ratio by treatment of the mixture with aqueous HCl at reflux temperatures appeared to have no effect. Finally, changing the solvent conditions of the reaction to a water−ethanol mixture strongly enhanced the formation of **10** with only trace amounts of the byproduct **12** detected. Using these modified conditions, the desired product **10** was successfully isolated in yields of 85% and its structure was confirmed by X-ray crystallography.

To further explore the formation of **12** in these reactions, a pure sample of **10** was heated at reflux in absolute ethanol containing a catalytic amount of HCl over a period of 24 h. Under these conditions, ~53% of the original sample of **10** was converted to **12**. This confirms that **12** is produced via nucleophilic attack of ethanol on **10**, rather than production directly from diamine **3**. It is thus believed that it is the enhanced ethanol solubility of **10** in comparison to the monomeric analogue **8**, as well as the presence of catalytic HCl, that is responsible for the difference in reactivity observed here. By moving to the more polar ethanol−water mixture, the solubility of **10** is reduced and therefore has less opportunity to react further to produce the unwanted byproduct **12**.

With the successful production of **10** accomplished, efforts turned to its conversion to the corresponding 2,3-dibromo-5,7-bis(2-thienyl)thieno[3,4-*b*]pyrazine (**5**) via the same conditions previously used for the conversion of **8** to **9**.[26] However, as with the production of **10** discussed above, the conditions that were successful for monomeric TPs did not translate well to the corresponding terthienyl analogues. As shown in Scheme 4, attempts to convert **10** to **5** resulted in very low yields with significant amounts of black insoluble material indicative of oxidative polymerization. Although the conditions applied in Scheme 4 had been previously optimized to reduce the decomposition of thiophene species via oxidative coupling and polymerization processes,[26] it is nearly impossible to eliminate such processes in the oxidative conditions of the PBr_5 mixtures

dx.doi.org/10.1021/jo400577q | J. Org. Chem. 2013, 78, 5453−5462

Scheme 4. Conversion of 10 to TP-Based Terthienyls with Good Leaving Groups

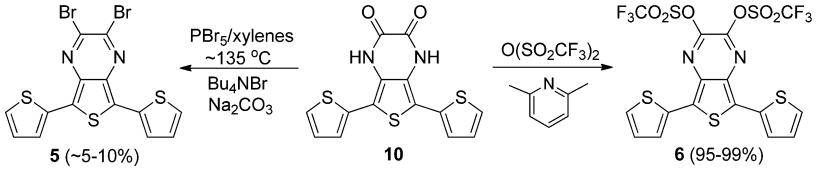

Scheme 5. Proposed Mechanism for the Formation of Terthienyl 6

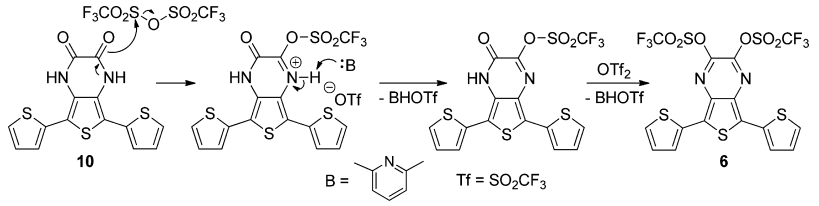

used. As terthienyls undergo oxidation at potentials nearly 1.0 V (~0.80−0.90 V)[2] lower than their corresponding monomeric analogues, decomposition via oxidative pathways becomes a much more significant problem in the case of the terthienyls **5** and **10**, which limits the successful isolation of the desired dihalo product **5** under these bromination conditions.

Due to the difficulties encountered with the isolation of **5**, alternate methods for the generation of TP-based terthienyls containing good leaving groups were then investigated. As a number of groups had reported the activation of amides with triflic anhydride to generate triflatoiminium triflate salts,[28−31] these conditions were then applied to **10** in an attempt to produce the ditriflato analogue **6** (Scheme 4). Typical conditions for such reactions utilize various pyridine bases to neutralize the triflic acid generated in this process, although the application of less bulky pyridines have been reported to undergo substitution reactions with the triflatoimine product to generate the pyridinium species.[30,31] In order to avoid such secondary reactions with the pyridine base, 2,6-lutidine was chosen as a less nucleophilic, yet cost-efficient base. Treatment of **10** with 2.2 equiv of triflic anhydride and 2.6 equiv of 2,6-lutidine successfully produced the desired ditriflato species **6** as a reactive, yet stable, purple solid in near-quantitative yields.

Based on previous mechanistic studies of such amide activations,[30] a proposed mechanism for the formation of **6** from **10** is given in Scheme 5. It is possible that the lutidine reacts first with the triflic anhydride to generate 2,6-dimethyl-*N*-(trifluoromethylsulfonyl)pyridinium triflate, by analogy to previously reported methods utilizing pyridine.[30] However, the reduced nucleophilic nature of the lutidine should inhibit or at least limit this process. If this pyridinium intermediate is produced, the proposed mechanism would deviate only in the exact identity of the electrophile in the initial step.

In order to explore the application of **6** to the production of new difunctionalized TP-based terthienyls, new analogues were generated as shown in Scheme 6. New TP-based terthienyls include the diethylamino species **13**, dihexyloxy species **14**, and the phenylalkynyl analogue **15**. All of these new TP-based terthienyls were produced in moderate to good yields by simple nucleophilic aromatic substitution of the triflate groups of **6**.

Lastly, to further expand the variety of functionality possible in TP-based terthienyls, the bis(bromomethyl) analogue **7** (Scheme 7) was produced via the room temperature condensation of diaminoterthiophene **3** with the commercially available 1,4-dibromo-2,3-butanedione. As in the case of **6** above, ether (**16a,b**) or amine (**17**) functionalities are then produced via simple substitution reactions.

Scheme 6. Generation of New TP-Based Terthienyls via Simple Substitution of 6

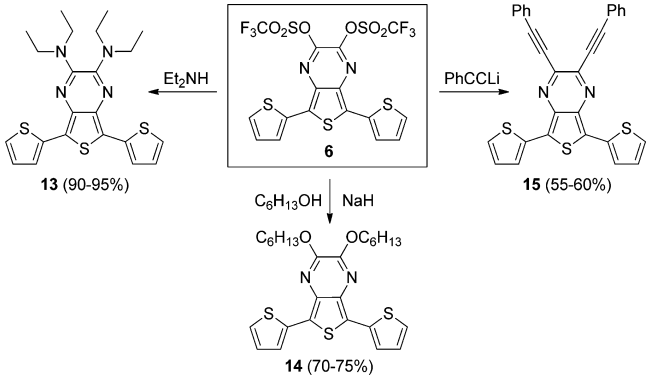

Scheme 7. Synthesis of New 2,3-Difunctionalized TP-Based Terthienyls from Precursor 7

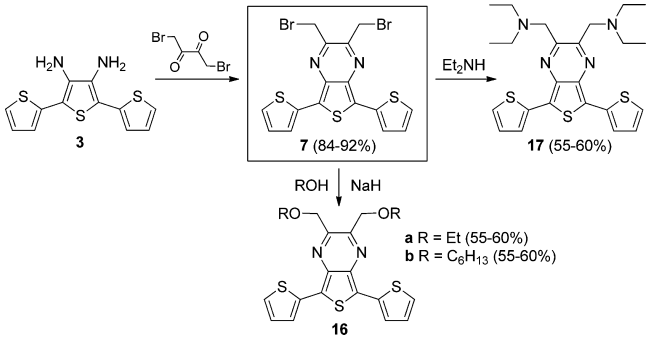

Crystallography. The X-ray quality crystals of the precursor dione **10** were grown from the slow evaporation of methanol solutions, and selected bond angles are given in Table 1. The pyrazine-2,3-dione ring of **10** represents a cyclic diamide which could potentially exist in multiple tautomeric forms as shown in Scheme 8. For typical amides, however, the equilibrium favors the amide tautomer almost exclusively over the iminol ($K = 10^8$),[32,33] regardless of the nature of any functional group bound to the carbonyl. For cyclic systems such as 4-hydroxypyrimide, in which the iminol form represents an aromatic system, one would expect greater iminol content. In

dx.doi.org/10.1021/jo400577q | J. Org. Chem. 2013, 78, 5453−5462

Table 1. Experimental Bond Lengths of 5,7-Bis(2-thienyl)thieno[3,4-*b*]pyrazine-2,3(1*H*,4*H*)-dione (10) and 2,3-Difunctionalized 5,7-Bis(2-thienyl)thieno[3,4-*b*]pyrazines 4b, 4e, 7, and 14

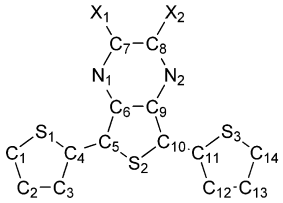

10 X = O
4b X = C
7 X = C-Br
14 X = O-C_6
4e X = C_{Ar}

bond	10	4b[a]	7	14	4e[b]
S(1)–C(4)	1.699(3)	1.719(5)	1.695(3)	1.727(2)	1.712(7)
C(1)–C(2)	1.360(4)	1.34(1)	1.343(4)	1.359(2)	1.32(1)
C(3)–C(4)	1.414(4)	1.424(7)	1.371(7)	1.422(2)	1.39(1)
C(2)–C(3)	1.443(3)	1.417(8)	1.488(8)	1.428(2)	1.41(1)
C(4)–C(5)	1.456(3)	1.442(7)	1.438(3)	1.445(2)	1.45(1)
S(2)–C(5)	1.727(3)	1.719(5)	1.733(2)	1.735(2)	1.713(6)
C(5)–C(6)	1.376(2)	1.406(7)	1.394(3)	1.380(2)	1.399(9)
C(6)–C(9)	1.420(4)	1.418(6)	1.426(3)	1.419(2)	1.427(9)
N(1)–C(6)	1.394(3)	1.381(6)	1.370(3)	1.382(2)	1.371(7)
N(1)–C(7)	1.355(2)	1.298(7)	1.311(3)	1.291(2)	1.313(9)
C(7)–C(8)	1.537(4)	1.469(7)	1.458(3)	1.469(2)	1.47(1)
C(7)–X(1)	1.222(3)	1.495(8)	1.489(3)	1.341(2)	1.489(7)

[a]Reference 5a. [b]Reference 16a.

Scheme 8. Possible Tautomeric Forms of Pyrazine-2,3-dione

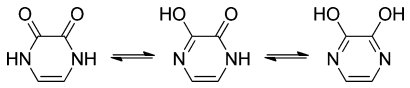

fact, this does seem to be true in the gas phase, where the equilibrium has been reported to be near unity, although the oxo form is again thought to predominate in either solution or the crystalline state.[34] For compound **10**, the combination of a cyclic system capable of an aromatic form and two different amide groups both able to undergo tautomerism could further favor the iminol form. However, this does not seem to be the case, and the determined solid-state structure of **10** appears to consist exclusively of the dione tautomer. The C–O bond lengths here are 1.222 and 1.226 Å, both slightly shorter than the typical C═O bond length of 1.23 Å.[35] While the C–N bond lengths (1.355 and 1.351 Å) exhibit some shortening in comparison to a pure C—N single bond (1.47 Å),[35] they are still longer than that reported for formamide (1.32 Å).[35] As such, the dione structure given in Schemes 3–5 seems to accurately represent the crystalline structure of **10**.

The X-ray quality crystals of the TP-based terthienyls **7** and **14** were also obtained, and selected bond lengths are given in Table 1, along with previously reported data from the analogues **4b**[5a] and **4e**[16a] for comparison. The bond lengths and angles of all four TP-based terthienyls are in fairly good agreement, and for the most part, the terthienyl backbones adopt a predominately s-trans configuration analogous to α-terthiophene.[36] Although the previously reported TP-based terthienyls exhibit nonplanar conjugated backbones in which the external thiophenes are rotated ∼10°–25° out of the plane of the central TP,[5a,16a] both **7** and **14** show near-planar geometries consistent with the structure of α-terthiophene. Terthienyl **14** exhibits torsion angles of 7.9° and 8.9°, similar to that of α-terthiophene (6°–9°),[36] while **7** exhibits a very planar backbone with torsion angles of only 0.7° and 1.2°.

Typical of monomeric TPs,[1,26] all four TP-based terthienyls exhibit some bond fixation with the fused pyrazine ring. For example, while the delocalized structure of the parent pyrazine heterocycle results in four equivalent C—N bonds, the fused pyrazine of TPs exhibits elongation of the thiophene-N bonds and shortening of the exterior C—N bonds of the pyrazine

Table 2. UV–visible Absorption Data for a Series of TP-Based Terthienyls[a]

	$S_0 \rightarrow S_1$ (ICT)			$S_0 \rightarrow S_2$ ($\pi \rightarrow \pi^*$)		
terthienyl	λ_{max} (nm)	ε (M^{-1} cm^{-1})	f	λ_{max} (nm)	ε ($M^{-1}cm^{-1}$)	f
4b	492	12100	0.242	339	21000	0.268
4f	540	7800	0.123	338	45100	0.908
5	542	7400	0.134	313	35400	1.391
6	556	*b*	*b*	337	*b*	*b*
7	544	7100	0.146	312	33300	1.012
13	404	11800	0.225	348	12800	0.163
14	444	10200	0.193	328	19000	0.390
15	586	4400	0.065	361	58000	1.327
16a	511	9600	0.192	339	21400	0.349
17	500	9600	0.197	338	19300	0.321

[a]In CH_3CN. [b]Accurate determination not possible due to reaction with solvent.

dx.doi.org/10.1021/jo400577q | J. Org. Chem. 2013, 78, 5453–5462

ring, i.e. N(1)—C(7). In the examples here, these exterior C—N bond lengths have an average length of 1.30 Å, nearly equivalent to that of localized C=N bonds (1.28 Å).[37] Comparison of the TP of **14** with the analogous bonds of **10** further illustrates the structural distinction between the diamide form of **10** and the dialkoxyaromatic ring of **14**. As expected, the N(1)—C(7) bond of **14** exhibits significant shortening in comparison to **10** (1.291 vs 1.355 Å). In addition, the C—O bond of **14** exhibits notable elongation relative to the C=O bond of **10** (1.341 vs 1.222 Å).

The external thiophenes of the TP-based terthienyls exhibit deviations from typical thiophene geometry due to positional disorder resulting from a portion of these heterocycles that are rotated 180° around the interannular bond, resulting in some mixing of the S1/C3 and S3/C12 positions. This is most pronounced in the structure of **7**, where positional disorder is observed in both external rings, resulting in approximately 17.32% mixing of the S1/C3 positions and 31.53% mixing of the S3/C12 positions. Terthienyl **14** exhibits disorder in only one of the two external thiophenes, resulting in mixing of approximately 7.43% for the S3/C12 positions. Other deviations include shortened external α,β-C−C bonds (i.e., C(1)−C(2) = 1.32−1.36 Å) in comparison to the parent thiophene (1.370 Å).[38] Both the positional disorder of the external thiophenes and the shortening of external α,β-C−C bonds have been previously observed for other oligothiophenes,[39−41] as well as the previous TP-based terthienyls **4b** and **4e**.[5a,16a]

UV−vis Spectroscopy. The spectral data of various TP-based terthienyls are given in Table 2, and a representative UV−vis spectrum of **4b** is shown in Figure 1. The absorption

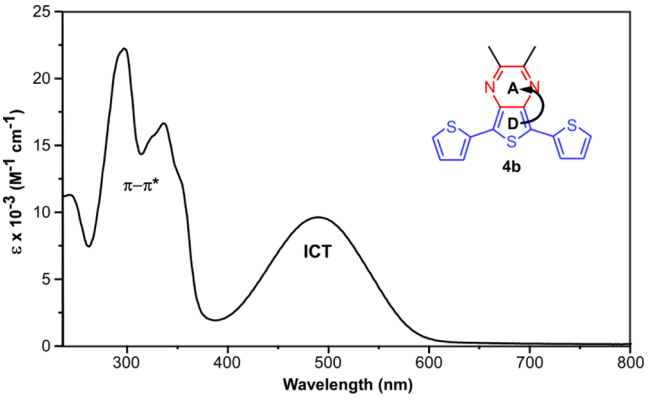

Figure 1. UV−visible spectrum of TP-based terthienyl **4b** in CH_3CN.

properties of the TP-based terthienyls are characterized by a broad, low energy transition, which is formally assigned as an intramolecular charge transfer (ICT) band. This assignment is consistent with previous photophysical studies that have shown that the lowest energy absorption of monomeric TPs is a broad ICT band resulting from a transition between a predominately thiophene-localized HOMO and a LUMO of greater pyrazine contribution.[1,26,42] For the TP-based terthienyls, the addition of the 2-thienyl groups to the 5- and 7-positions of the TP unit results in a HOMO which is now delocalized across the terthienyl backbone, while still retaining a LUMO dominated by pyrazine contributions (Figure 1). The ICT nature of this low energy transition also accounts for the significant red shift observed for dialkyl-functionalized TP-based terthienyls in comparison to the parent α-terthiophene (492 vs 354 nm).[43]

As can be seen in Table 2, the extinction coefficients and oscillator strengths of these transitions are somewhat low. This is due to a reduced "allowedness" of the transition as a result of limited spatial overlap of the orbitals involved in the ICT transition.[44]

Two stronger sets of bands are exhibited in the higher-energy region of 250−350 nm, which are assigned as two $\pi\rightarrow\pi^*$ transitions localized primarily on the terthienyl backbone. As would thus be expected, the energies of these transitions agree well with the absorption energies reported for α-terthiophene.[43] For the most part, the extinction coefficients for these $\pi\rightarrow\pi^*$ bands fall roughly between 20×10^3 and 58×10^3 M^{-1} cm^{-1}, with corresponding oscillator strengths of approximately 0.30−1.30 and ranging from moderately allowed to fully allowed transitions.

Overall, the effect of the side chains in the TP-based terthienyls is similar to that previously reported for the monomeric analogues,[26] although with some significant differences. As shown in both Table 2 and the absorption spectra in Figure 2, the HOMO−LUMO energy, and thus the

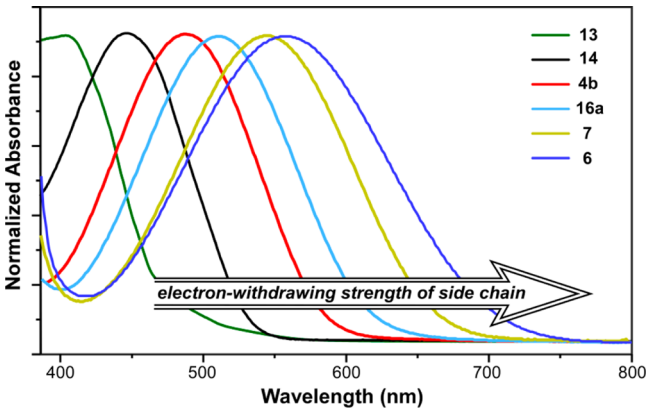

Figure 2. Normalized visible spectra of a series of TP-based terthienyls.

energy of the ICT transition, decreases as the electron-withdrawing nature of the side chain increases. Thus, by simply changing the identity of the side chains of the TP-based terthienyls reported here, it is possible to shift the λ_{max} of the ICT transition by over 180 nm. When presented as such in terms of wavelength, this extent of tuning appears even greater than that previously reported for the simple TP monomeric analogues.[26] However, when viewed in terms of a linear electronvolt scale, the changes in energy are actually similar (~0.9 vs 1.1 eV).

Electrochemistry. The electrochemical data of the TP-based terthienyls are given in Table 3, and a representative cyclic voltammogram is shown in Figure 3. Typical of monomeric TPs,[26,45] the TP-based terthienyls exhibit a well-defined irreversible oxidation assigned to the oxidation of the terthiophene backbone, as well as a quasireversible pyrazine-based reduction. As for the majority of thiophene species, the irreversible nature of the oxidation here is due to the formation of thiophene-based radical cations. The rapid coupling of these radical cations then results in higher oligomeric and polymeric species, which accounts for the observed irreversibility. It should also be noted that, for terthienyls **13** and **17**, the alkylamino side chains are also redox active, and thus oxidations of both the amine functionality and the thiophene are observed.

dx.doi.org/10.1021/jo400577q | J. Org. Chem. 2013, 78, 5453−5462

Table 3. Electrochemical Data for a Series of TP-Based Terthienyls[a]

	oxidation	reduction	
terthienyl	E_p^a, V	$E_{1/2}$, V	ΔE, mV
4b	0.50	−1.68	100
4f	0.54	−1.46	60
5	0.70	−1.14[b]	–
6	0.80	−0.99[b]	–
7	0.62	−1.26	160
13	−0.06,[c] 0.24	*nwsw*	–
14	0.45	−2.03	90
15	0.59	−0.96[b]	–
16a	0.57	−1.48	110
16b	0.57	−1.48	120
17	0.32,[c] 0.62	−1.65	90

[a]All potentials vs Ag/Ag^+. *nwsw* = not within solvent window. [b]Irreversible; value corresponds to E_p^c. [c]Nitrogen-based oxidation.

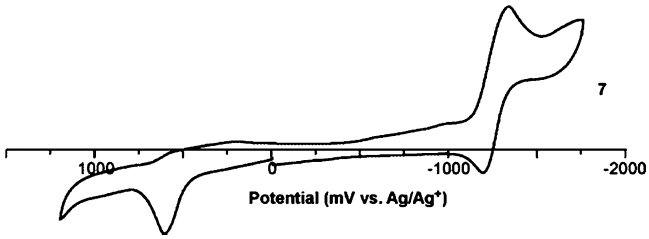

Figure 3. Cyclic voltammogram of terthienyl 7.

In these cases, the initial oxidation is that of the amine, as previously observed in the electrochemistry reported for 2,3-di(*N*-decylamino)thieno[3,4-*b*]pyrazine[26] and the related 3-(*N*-alkylamino)thiophenes.[46]

As previously seen for monomeric TPs,[26] the potential of oxidation becomes more positive as the electron-withdrawing nature of the side chain is increased, indicative of a stabilization of the HOMO. With the exception of terthienyls **5** and **6**, however, all of the TP-based terthienyls reported here still undergo oxidation at lower potentials than the parent α-terthiophene (0.65 V vs Ag/Ag^+).[47] As might be expected, the effect on the reduction potentials follows the opposing trend, with electron-withdrawing groups reducing the potential to as low as −0.99 V. Likewise, electron-donating groups increase the potential to the extent that the reduction of TP-based terthienyls with strongly donating groups such as dialkylamino are no longer within the measurable solvent windows of CH_3CN. For terthienyl **15**, an additional sharp irreversible oxidation was observed at −60 mV after cycling through the reduction at ∼−1 V. While the nature of this additional redox process is currently unknown, it is believed that this may be the result of a redox-initiated 1,5-cyclization of the enediyne structure. Similar cyclizations of enediynes via both oxidation[48,49] and reduction[50] processes have been previously reported, and a separate study of the electrochemical, photochemical, and thermal cyclization of **15** is planned.

While the side chain effect on the reduction potentials of the TP-based terthienyls is essentially the same as that previously seen with the monomeric TPs, the effect on the potential of oxidation is significantly attenuated in the terthienyl analogues. For example, changing the functional groups of monomeric TPs from the hexyloxy to methylbromo results in nearly a 300 mV shift in the potential of oxidation.[26] In comparison, the same exact change in the TP-based terthienyls results in only a shift of 170 mV. This difference is due to the fact that the effect of the two additional 2-thienyl groups in the terthienyls contributes more significantly to the HOMO than the functional groups at the 2- and 3-positions of the TP unit. This results in delocalization of the HOMO across the terthienyl backbone and significant destabilization of the HOMO energy, as illustrated by a shift in the potential of oxidation by 850 mV from monomeric TP to TP-based terthienyl.[26,45] Thus the side chain effects of the central TP unit are diluted across the large conjugated backbone such that the destabilization of the HOMO by the added external thiophenes effectively overpowers the weaker contribution of the TP side chains.

The variations in the potentials of both oxidation and reduction of the TP-based terthienyls correlate well with the respective Hammett substituent constants (σ_p^+ or σ_p^-) as shown in Figure 4. The shifts in redox potentials of comparable

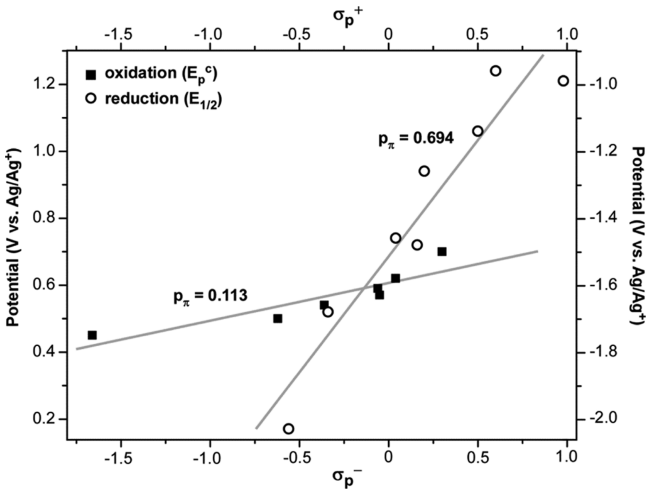

Figure 4. Hammet plot of TP-based terthienyls.

molecular species are dependent on the polar, steric, and mesomeric effects exerted by the substituents as described by the Hammett−Taft equation:

$$E = \rho_\pi \sigma + S$$

where $\rho_\pi\sigma$ describes the polar-mesomeric parameters and S accounts for the steric factors.[26,46,51−53] In cases of low or comparable steric interactions as a result of the added functional groups (i.e., S is constant), linear relationships are found between the potential of oxidation and σ_p^+ (or the reduction potential and σ_p^-).

As seen in Figure 4, both plots (oxidation vs σ_p^+ and the reduction vs σ_p^-) give linear relationships with respective R values of 0.900 and 0.953. In terms of the potential of oxidation, the plot gives a ρ_π value of 0.113, exactly one-third of that previously found for the corresponding monomeric thieno[3,4-*b*]pyrazines (ρ_π= 0.340)[26] and significantly lower than that for typical thiophenes (ρ_π = 0.80).[51] The lower ρ_π values for both sets of thieno[3,4-*b*]pyrazine compounds is indicative of the diminished effect of the functional group on the potential of oxidation in these species. This lower effect is expected as the functional groups are spatially removed from the site of oxidation localized either on the thiophene ring of the TP unit or across the terthienyl backbone. As the oxidation

dx.doi.org/10.1021/jo400577q | J. Org. Chem. 2013, 78, 5453−5462

of the TP-terthienyls is delocalized across the terthienyl backbone, the one-third reduction in the side chain effects is perfectly consistent with the fact that only one-third of that backbone is comprised of a functionalized TP.

The plot of the reduction potentials of the TP-based terthienyls gives a higher value of $\rho_\pi = 0.694$, indicating a higher effect of the functional group on the TP reduction as expected. What was unexpected, however, is that this value is considerably larger than that previously found for the monomeric thieno[3,4-*b*]pyrazines ($\rho_\pi = 0.463$).[26] As the side chain contribution to the pyrazine ring should be identical between the monomers and the TP-based terthienyls, the ρ_π values should be fairly consistent. Re-evaluation of the original thieno[3,4-*b*]pyrazine data[26] indicates that one outlying data point for the 2,3-dicyanothieno[3,4-*b*]pyrazine monomer is responsible for the skewing of the determined slope. Removal of this data point results in a newly calculated ρ_π value of 0.613 for the TP monomers, which is now in good agreement with the TP-based terthienyls studied here. The cause of the poor correlation for the 2,3-dicyanothieno[3,4-*b*]pyrazine[26] monomer is currently unknown, and its electrochemistry may need to be restudied in greater detail.

■ CONCLUSIONS

New classes of TP-based terthienyls containing electron-donating and -withdrawing groups have been prepared from terthienyls containing central 2,3-ditriflato- and 2,3-bis(bromomethyl)thieno[3,4-*b*]pyrazines. As previously demonstrated for thieno[3,4-*b*]pyrazine monomers,[26] the ability to vary the functional groups allows significant tuning of the electronic and optical properties of these popular conjugated building blocks. The additional terminal thiophenes of the TP-based terthienyls reduce the effect of the functional groups on the modulation of the HOMO energies by approximately one-third in comparison to that of the TP monomers, while having essentially no effect on the modulation of the corresponding LUMO energies. As such, the tuning ability of these TP-based terthienyls complements that of the TP monomers and provides a promising new class of building blocks for the production of new low band gap materials.

■ EXPERIMENTAL SECTION

Materials. 2,5-Dibromo-3,4-dinitrothiophene (**1**),[33] tributyl(2-thienyl)stannane,[54] 2,3-dimethyl-5,7-bis(2-thienyl)thieno[3,4-*b*]-pyrazine (**4b**),[5b] 2,3-diphenyl-5,7-bis(2-thienyl)thieno[3,4-*b*]pyrazine (**4f**),[14a] and PBr_5[55] were all prepared as previously reported. Xylenes and THF were distilled from sodium/benzophenone prior to use. CH_2Cl_2 and CH_3CN were dried over CaH and distilled prior to use. DMF was dried over $MgSO_4$ prior to use. All other materials were reagent grade and used without further purification.

3′,4′-Dinitro-2,2′:5′,2″-terthiophene (2). The following is a modification of previously reported methods.[5b] Compound **1** (17.2 g, 51.8 mmol) and tributyl(2-thienyl)stannane (42.51 g, 114 mmol) were added to dry THF (250 mL), followed by the addition of $PdCl_2(PPh_3)_2$ (0.364 g, 1 mol %). The mixture was heated to reflux for 16 h. After cooling, the reaction mixture was concentrated under vacuum to approximately 50 mL. Hexanes were then added, and the resulting orange precipitate was filtered and washed with hexanes. The solid was recrystallized in methanol and purified by silica chromatography (gradient of hexanes to 20% CH_2Cl_2 in hexanes) to give 12.3−13.1 g (70−75%). Mp 144−145 °C (lit.[5b]149−151 °C). ^{1}H NMR: δ 7.61 (dd, J = 1.2, 5.2 Hz, 2H), 7.55 (dd, J = 1.2, 3.6 Hz, 2H), 7.18 (dd, J = 3.6, 5.2 Hz, 2H); ^{13}C NMR: δ 136.2, 134.1, 131.5, 131.4, 128.6, 128.3.

3′,4′-Diamino-2,2′:5′,2″-terthiophene (3). The following is a modification of previously reported methods.[5b] Terthiophene **2** (13.5 g, 40.0 mmol) was suspended in a mixture of ethanol (340 mL) and concentrated HCl (280 mL). Tin metal (45.6 g, 384 mmol) was then added slowly in small portions, and the mixture stirred at room temperature for 72 h. The mixture was then cooled to −25 °C and filtered, and the isolated solid was washed with diethyl ether. The light green diammonium salt was added to 400 mL of cold water and made basic with 1 M KOH. The basic solution was then extracted with CH_2Cl_2 until no color was observed in the extract. The combined organics were dried with $MgSO_4$, filtered, and concentrated under vacuum. The crude product was purified by silica chromatography (gradient $CHCl_3$ to 5% triethylamine in $CHCl_3$) to give 8.4−8.9 g of a yellow-brown powder (75−80%). Mp 90−92 °C (lit.[5b]96.0−96.5 °C). ^{1}H NMR: δ 7.25 (dd, J = 1.2, 3.6 Hz, 2H), 7.07 (m, 4H), 3.71 (s, 4H). ^{13}C NMR: δ 136.2, 133.8, 128.0, 124.2, 124.1, 110.4. All NMR values agree with previously reported values.[5b]

5,7-Bis(2-thienyl)thieno[3,4-*b*]pyrazine-2,3(1*H*,4*H*)-dione (10). Diamine **3** (1.39 g, 5.0 mmol) was added to 120 mL of a 1:1 ethanol/water mixture under a nitrogen atmosphere. Diethyl oxalate (5.98 mL, 44 mmol) and concentrated HCl (0.20 mL, 6.5 mmol) were then added and heated at reflux for 24 h. The mixture was then cooled to room temperature, and the ethanol was removed under vacuum. The remaining mixture was then cooled in a freezer, after which the resulting precipitate was collected via vacuum filtration and washed with water (300 mL). The collected solid was then dissolved in 1 M aqueous KOH (500 mL) and filtered to remove any undissolved material. The KOH solution was then made acidic, and the resulting precipitate was collected via vacuum filtration. The solid was washed with water (∼100 mL) and then diethyl ether until dry to produce 1.33−1.41 g of a yellow powder (80−85%). Mp 216 °C dec. ^{1}H NMR: δ 7.17 (m, 4H), 7.46 (dd, J = 2.0, 4.4 Hz, 2H), 8.68 (br, 2H); ^{13}C NMR (*d*-DMSO): δ 159.1, 136.4, 133.9, 133.2, 132.6, 129.3, 115.6; HRMS m/z 354.9642 $[M + Na]^+$ (calcd for $C_{14}H_8N_2NaO_2S_3$ 354.9640).

2,3-Dibromo-5,7-bis(2-thienyl)thieno[3,4-*b*]pyrazine (5). The reagents PBr_5 (0.32 g, 0.75 mmol), Bu_4NBr (0.19 g, 0.60 mmol), and Na_2CO_3 (0.06 g, 0.6 mmol) were added to 50 mL of xylenes in a 100 mL round-bottom flask equipped with a Vigreaux column. This column was then fitted with a condenser, with an outlet submerged in 2.5 M aqueous KOH solution. The entire assembly was maintained under a gentle stream of nitrogen. The reaction mixture was then heated to reflux, which resulted in a color change from deep red to light yellow-orange. Compound **10** (0.10 g, 0.30 mmol) was then added, and the reaction was allowed to stir at reflux overnight. The reaction was quenched with a saturated aqueous NH_4Cl solution (100 mL) and extracted with CH_2Cl_2 (3 × 50 mL). The combined organic layers were dried with anhydrous $MgSO_4$, concentrated, and purified by column chromatography (2% CH_2Cl_2 in hexanes) to give ∼10 mg of a purple solid (<10% yield). ^{1}H NMR: δ 7.64 (dd, J = 1.1, 3.7 Hz, 2H), 7.42 (dd, J = 1.1, 5.1 Hz, 2H), 7.13 (dd, J = 3.7, 5.1 Hz, 2H).

5,7-Bis(2-thienyl)-2,3-bis(trifluoromethanesulfonato)thieno-[3,4-*b*]pyrazine (6). Dione **10** (1.10 g, 3.3 mmol) was added to a flask under a nitrogen atmosphere, which was then charged with 2,6-lutidine (0.92 g, 8.6 mmol) and dry CH_2Cl_2 (150 mL) and cooled to −10 °C in an ice/salt bath. Once cooled, trifluoromethanesulfonic anhydride (7.26 mL, 1.0 M in CH_2Cl_2, 7.26 mmol) was added dropwise over 1 h to limit heat evolution. The reaction was then quenched with saturated aq. $NaHCO_3$ (200 mL) and extracted with CH_2Cl_2 (3 × 100 mL). The combined organics were dried with $MgSO_4$, filtered, and concentrated. The crude product was purified by silica chromatography (1:1 CH_2Cl_2/hexanes) to give 1.87−1.95 g of a purple solid (95−99%). Mp 174 °C dec. ^{1}H NMR: δ 7.63 (dd, J = 1.2, 3.6 Hz, 2H), 7.47 (dd, J = 1.2, 5.2 Hz, 2H), 7.15 (dd, J = 3.6, 5.2 Hz, 2H); ^{13}C NMR: δ 139.8, 133.1, 132.7, 128.4, 126.7, 128.1, 127.5, 126.6, 118.7 (q, J_{C-F} = 300 Hz); HRMS m/z 618.8601 $[M + Na]^+$ (calcd for $C_{16}H_6F_6N_2O_6S_5Na$ 618.8626).

2,3-Bis(*N*,*N*-diethylamino)-5,7-bis(2-thienyl)thieno[3,4-*b*]-pyrazine (13). Ditriflate **6** (0.190 g, 0.32 mmol) was added to a flask and brought under a nitrogen atmosphere. Dry CH_2Cl_2 (40 mL) was

dx.doi.org/10.1021/jo400577q | J. Org. Chem. 2013, 78, 5453−5462

added, followed by the addition of *N,N*-diethylamine (10.0 mL, 193 mmol). The reaction was allowed to stir at room temperature overnight, after which it was quenched with saturated aq. $NaHCO_3$ (100 mL) and extracted with CH_2Cl_2 (3 × 50 mL). The combined organics were dried with $MgSO_4$, filtered, and concentrated. The crude product was purified by basic silica chromatography (prepared with 80:20 hexanes/CH_2Cl_2 containing 3% triethylamine, eluted with hexanes/CH_2Cl_2) to give 0.13−0.14 g of a shiny red-orange solid (90−95%). Mp 106−109 °C. ^{1}H NMR: δ 7.43 (dd, J = 1.2, 3.6 Hz, 2H), 7.27 (dd, J = 1.2, 5.2 Hz, 2H), 7.06 (dd, J = 3.6, 5.2 Hz, 2H), 3.64 (q, J = 7.1 Hz, 8H), 1.17 (t, J = 7.1 Hz, 12H); ^{13}C NMR: δ 12.9, 43.9, 118.3, 122.2, 124.8, 126.9, 135.8, 136.3, 148.6; HRMS m/z 443.1393 $[M + H]^+$ (calcd for $C_{22}H_{26}N_4S_3H$ 443.1392).

2,3-Dihexyloxy-5,7-bis(2-thienyl)thieno[3,4-*b*]pyrazine (14). Sodium hexyloxide was prepared by the addition of NaH (0.20 g, 5.0 mmol, 60−65% in oil) to a flask under a nitrogen atmosphere. The oil was removed by washing with hexanes (2 × 10 mL), and the remaining NaH was brought to dryness under vacuum. The flask was then equipped with an addition funnel charged with ditriflate **6** (0.298 g, 0.5 mmol) in 50 mL of dry CH_2Cl_2, after which dry DMF (50 mL) was added to the reaction flask. The reaction was cooled to −15 °C in an ice/salt bath, and 1-hexanol (1.0 mL, 8 mmol) was added to the DMF solution and allowed to stir for 1 h. The solution of **6** was then added dropwise while maintaining a temperature below −10 °C. Once the addition was complete, the reaction was allowed to warm to room temperature and stirred overnight. Saturated aqueous NH_4Cl (100 mL) was then added, and the mixture was extracted with CH_2Cl_2 (3 × 100 mL). The combined organics were dried with $MgSO_4$, filtered, and concentrated. The crude product was purified by silica chromatography (hexanes/CH_2Cl_2, 95:5) to give 0.18−0.20 g of an orange solid (70−75%). Mp 113−115 °C. ^{1}H NMR: δ 7.44 (dd, J = 1.2, 3.0 Hz, 2H), 7.30 (dd, J = 1.2, 4.5 Hz, 2H), 7.05 (dd, J = 3.0, 4.5 Hz, 2H), 4.55 (t, J = 7.0 Hz, 4H), 1.91 (p, J = 7.0 Hz, 4H), 1.49 (p, J = 7.0 Hz, 4H), 1.36 (m, 8H), 0.90 (t, J = 7.0 Hz, 6H); ^{13}C NMR: δ 150.3, 135.4, 134.1, 127.1, 125.5, 123.3, 120.5, 68.1, 31.8, 28.5, 26.0, 22.8, 14.2. All NMR values agree with previously reported values;[27] HRMS m/z 551.1846 $[M + Na]^+$ (calcd for $C_{28}H_{36}N_2O_2S_3Na$ 551.1831).

2,3-Bis(phenylethynyl)-5,7-bis(2-thienyl)thieno[3,4-*b*]pyrazine (15). Phenylacetylene (0.064 g, 0.625 mmol) was added to a flask under nitrogen and cooled to 0 °C. Once cool, butyl lithium (0.25 mL, 0.625 mmol, 2.5 M in hexanes) was added dropwise and the reaction was allowed to stir for 30 min. In a separate flask, ditriflate **6** (0.149 g, 0.25 mmol) was dissolved in 50 mL of THF and cooled to 0 °C in an ice bath. The lithium phenylacetylide solution was then added dropwise to the solution of **6**, after which the mixture was allowed to warm to room temperature and stirred overnight. The THF was then removed under vacuum, 100 mL of saturated aq. NH_4Cl were added, and the mixture was extracted with CH_2Cl_2 (3 × 50 mL). The combined organics were dried with $MgSO_4$, filtered, and concentrated. The crude product was purified by silica chromatography (prepared with 100% hexanes, eluted with 70:30 hexanes/CH_2Cl_2) to give 69−75 mg of a dark blue solid (55−60%). Mp 206−209 °C. ^{1}H NMR: δ 7.72 (d, J = 3.6 Hz, 2H), 7.68 (d, J = 6.5 Hz, 4H), 7.41 (m, 8H), 7.14 (dd, J = 3.6, 5.2 Hz, 2H); ^{13}C NMR: δ 140.0, 136.6, 132.6, 129.9, 128.7, 127.8, 127.3, 125.9, 125.8, 122.1, 96.5, 87.9; HRMS m/z 523.0383 $[M + Na]^+$ (calcd for $C_{30}H_{16}N_2S_3Na$ 523.0368).

2,3-Bis(bromomethyl)-5,7-bis(2-thienyl)thieno[3,4-*b*]pyrazine (7). The following is a modification of previously reported methods.[27] Diamine **3** (1.39 g, 5.0 mmol) was added to absolute ethanol (80 mL) and gently heated with stirring until completely dissolved, after which it was allowed to cool to room temperature. In a similar manner, 1,4-dibromo-2,3-butanedione (1.89 g, 7.5 mmol) was added to absolute ethanol (40 mL), gently heated with stirring until completely dissolved, and allowed to cool to room temperature. The dione solution was then added dropwise to the solution of **3**, and the mixture was allowed to stir for 6 h, during which precipitation of the product occurred. The mixture was then cooled to −25 °C in a freezer (ca. 1 h), filtered, and washed with cold ethanol to give 2.03−2.23 g of a purple solid (84−92%). Mp 160 °C dec. ^{1}H NMR: δ 7.66 (dd, J = 1.2, 3.6 Hz, 2H), 7.39 (dd, J = 1.2, 5.2 Hz, 2H), 7.11 (dd, J = 3.6, 5.2 Hz, 2H), 4.86 (s); ^{13}C NMR: δ 150.1, 137.5, 134.1, 127.7, 127.4, 126.3, 125.7, 31.6. NMR values agree with previously reported values;[27] HRMS m/z 506.8290 $[M + Na]^+$ (calcd for $C_{16}H_{10}Br_2N_2S_3Na$ 506.8265).

General Synthesis of 2,3-Dialkoxymethyl-5,7-bis(2-thienyl)-thieno[3,4-*b*]pyrazine. Sodium alkoxide was prepared by addition of NaH (0.40 g, 10.0 mmol, 60−65% in oil) to 20 mL of the specified alcohol, and the mixture was stirred for 2 h to ensure complete NaH consumption. The alkoxide solution was then added dropwise to **7** (0.49 g, 1.0 mmol) in 50 mL of dry CH_2Cl_2, and the mixture allowed to stir for 6 h. Saturated aq. NH_4Cl was then added, and the CH_2Cl_2/alcohol solvents were removed by rotary evaporation and vacuum distillation as needed. The aqueous mixture was then extracted with CH_2Cl_2, after which the combined organic fractions were dried with $MgSO_4$ and concentrated.

2,3-Bis(ethoxymethyl)-5,7-bis(2-thienyl)thieno[3,4-*b*]-pyrazine (16a). Purified by silica chromatography (100% CH_2Cl_2) to give 0.24−0.26 g of a red/purple solid (55−60%). Mp 84−86 °C. ^{1}H NMR: δ 7.64 (dd, J = 1.2, 3.6 Hz, 2H), 7.36 (dd, J = 1.2, 5.2 Hz, 2H), 7.09 (dd, J = 3.6, 5.2 Hz, 2H), 4.86 (s, 4H), 3.67 (q, J = 6.8 Hz, 4H), 1.27 (t, J = 6.8 Hz, 6H); ^{13}C NMR: δ 152.3, 137.7, 134.6, 127.5, 126.8, 125.4, 125.0, 72.6, 66.7, 15.5; HRMS m/z 439.0581 $[M + Na]^+$ (calcd for $C_{20}H_{20}N_2O_2S_3Na$ 439.0579).

2,3-Bis(hexyloxymethyl)-5,7-bis(2-thienyl)thieno[3,4-*b*]-pyrazine (16b). Purified by silica chromatography (50% CH_2Cl_2/hexanes) to give 0.29−0.32 g of a red-purple solid (55−60%). ^{1}H NMR: δ 7.64 (dd, J = 1.2, 3.6 Hz, 2H), 7.36 (dd, J = 1.2, 5.2 Hz, 2H), 7.09 (dd, J = 3.6, 5.2 Hz, 2H), 4.86 (s, 4H), 3.62 (t, J = 6.8 Hz, 4H), 1.68 (p, J = 6.8 Hz, 4H), 1.39 (m, 4H), 1.30 (m, 8H), 0.89 (t, J = 6.8 Hz, 6H); ^{13}C NMR: δ 152.4, 137.7, 134.6, 127.5, 126.7, 125.4, 125.0, 72.8, 71.6, 31.9, 30.0, 26.1, 22.8, 14.3; HRMS m/z 551.1846 $[M + Na]^+$ (calcd for $C_{28}H_{36}N_2NaO_2S_3$ 551.1831).

2,3-Bis(*N,N*-diethylaminomethyl)-5,7-bis(2-thienyl)thieno-[3,4-*b*]pyrazine (17). Terthienyl **7** (0.24 g, 0.5 mmol) was added to dry CH_2Cl_2 (25 mL), followed by the dropwise addition of *N,N*-diethylamine (25 mL, 242 mmol). The reaction was heated at reflux for 5 h. It was then quenched with distilled H_2O and extracted with CH_2Cl_2 (3 × 50 mL). The combined organics were washed with saturated aq. $NaHCO_3$ (2 × 100 mL) and brine (2 × 100 mL), dried with $MgSO_4$, filtered, and concentrated. The crude product was purified by basic silica chromatography (prepared with 3% triethylamine/CH_2Cl_2, eluted with 100% CH_2Cl_2) to give 0.13−0.14 g of a dark red solid (55−60%). Mp 63−66 °C. ^{1}H NMR: δ 7.63 (dd, J = 1.2, 3.6 Hz, 2H), 7.36 (dd, J = 1.2, 5.2 Hz, 2H), 7.09 (dd, J = 3.6, 5.2 Hz, 2H), 4.10 (s, 4H), 2.73 (q, J = 7.2 Hz, 8H), 1.06 (t, J = 7.2 Hz 12H); ^{13}C NMR: δ 154.6, 137.7, 135.0, 127.3, 126.5, 124.6, 124.5, 57.5, 46.6, 11.4; HRMS m/z 471.1707 $[M + H]^+$ (calcd for $C_{24}H_{31}N_4S_3$ 471.1705).

UV−visible Spectroscopy. UV−visible spectra were measured on a dual beam scanning spectrophotometer using samples prepared as dilute CH_3CN solutions in 1 cm quartz cuvettes. Oscillator strengths were determined from the visible spectra via spectral fitting to accurately quantify the area of each transition and then calculated using literature methods.[56]

Electrochemistry. All electrochemical methods were performed utilizing a three-electrode cell consisting of a platinum disc working electrode, a platinum wire auxiliary electrode, and a Ag/Ag^+ reference electrode (0.251 V vs SCE).[57] The supporting electrolyte consisted of 0.10 M tetrabutylammonium hexafluorophosphate ($TBAPF_6$) in dry CH_3CN. Solutions were deoxygenated by sparging with argon prior to each scan and blanketed with argon during the measurements. All measurements were collected at a scan rate of 100 mV/s.

■ ASSOCIATED CONTENT

Supporting Information

NMR spectra for **5**−**7**, **10**, **13**−**17**; crystallographic data for **7**, **10**, **14**; and full UV−visible data. This material is available free of charge via the Internet at http://pubs.acs.org.

dx.doi.org/10.1021/jo400577q | J. Org. Chem. 2013, 78, 5453−5462

AUTHOR INFORMATION

Corresponding Author

*E-mail: seth.rasmussen@ndsu.edu.

Notes

The authors declare no competing financial interest.

ACKNOWLEDGMENTS

The authors thank the National Science Foundation (DMR-0907043) and North Dakota State University for support of this research and NSF-CRIF (CHE-0946990) for the purchase of the departmental XRD instrument. We wish to thank Dr. Angel Ugrinov for assistance with the collection of the X-ray crystal data.

REFERENCES

(1) Rasmussen, S. C.; Mulholland, M. E.; Schwiderski, R. L.; Larsen, C. A. *J. Heterocycl. Chem.* **2012**, *49*, 479.

(2) Rasmussen, S. C.; Schwiderski, R. L.; Mulholland, M. E. *Chem. Commun.* **2011**, *47*, 11394.

(3) Rasmussen, S. C.; Pomerantz, M. In *The Handbook of Conducting Polymers*, 3rd ed.; Skotheim, T. A., Reynolds, J. R., Eds.; CRC Press: Boca Raton, FL, 2007; Vol. *1*, Chapter 12.

(4) Rasmussen, S. C.; Ogawa, K.; Rothstein, S. D. In *the Handbook of Organic Electronics and Photonics*; Nalwa, H. S., Ed.; American Scientific Publishers: Stevenson Ranch, CA, 2008; Vol. *1*, Chapter 1.

(5) (a) Kitamura, C.; Tanaka, S.; Yamashita, Y. *J. Chem. Soc., Chem. Commun.* **1994**, 1585. (b) Kitamura, C.; Tanaka, S.; Yamashita, Y. *Chem. Mater.* **1996**, *8*, 570. (c) Delgado, M. C. R.; Hernandez, V.; Navarrete, J. T. L.; Tanaka, S.; Yamashita, Y. *J. Phys. Chem. B* **2004**, *108*, 2516.

(6) Zhu, Z.; Champion, R. D.; Jenekhe, S. A. *Macromolecules* **2006**, *39*, 8721.

(7) Wen, L.; Rasmussen, S. C. *J. Chem. Crystallogr.* **2007**, *37*, 387.

(8) Xia, Y.; Luo, J.; Deng, X.; Li, X.; Li, D.; Zhu, X.; Yang, W.; Cao, Y. *Macromol. Chem. Phys.* **2006**, *207*, 511.

(9) Karsten, B. P.; Viani, L.; Gierschner, J.; Cornil, J.; Janssen, R. A. J. *J. Phys. Chem. A* **2008**, *112*, 10764.

(10) Lee, W.; Cheng, K.; Wang, T.; Chueh, C.; Chen, W.; Tuan, C.; Lin, J. *Macromol. Chem. Phys.* **2007**, *208*, 1919.

(11) Liu, C.; Tsai, J.; Lee, W.; Chen, W.; Jenekhe, S. A. *Macromolecules* **2008**, *41*, 6952.

(12) Zhou, E.; Cong, J.; Yamakawa, S.; Wei, Q.; Nakamura, M.; Tajima, K.; Yang, C.; Hashimoto, K. *Macromolecules* **2010**, *43*, 2873.

(13) Chao, C.; Lim, H.; Chao, C. *Polym. Prepr.* **2010**, *51* (1), 715.

(14) (a) Perzon, E.; Wang, X.; Zhang, F.; Mammo, W.; Delgado, J. L.; de la Cruz, P.; Inganas, O.; Langa, F.; Andersson, M. R. *Synth. Met.* **2005**, *154*, 53. (b) Zhang, F.; Perzon, E.; Wang, X.; Mammo, W.; Andersson, M. R.; Inganas, O. *Adv. Funct. Mater.* **2005**, *15*, 745. (c) Admassie, S.; Inganas, O.; Mammo, W.; Perzon, E.; Andersson, M. R. *Synth. Met.* **2006**, *156*, 614. (d) Cai, T.; Zhou, Y.; Wang, E.; Hellstrom, S.; Zhang, F.; Xu, S.; Inganas, O.; Andersson, M. R. *Sol. Energy Mater. Sol. Cells* **2010**, *94*, 1275. (e) Tehrani, P.; Isaksson, J.; Mammo, W.; Andersson, M. R.; Robinson, N. D.; Berggren, M. *Thin Solid Films* **2006**, *515*, 2485.

(15) (a) Wienk, M. M.; Turbiez, M. G. R.; Struijk, M. P.; Fonrodona, M.; Janssen, R. A. J. *Appl. Phys. Lett.* **2006**, *88*, 153511. (b) Zoombelt, A. P.; Fonrodona, M.; Turbiez, M. G. R.; Wienk, M. M.; Janssen, R. A. J. *J. Mater. Chem.* **2009**, *19*, 5336. (c) Zoombelt, A. P.; Leenen, M. A. M.; Fonrodona, M.; Nicholas, Y.; Wienk, M. M.; Janssen, R. A. J. *Polymer* **2009**, *50*, 4564.

(16) (a) Petersen, M. H.; Hagemann, O.; Nielsen, K. T.; Jorgensen, M.; Krebs, F. C. *Sol. Energy Mater. Sol. Cells* **2007**, *91*, 996. (b) Petersen, M. H.; Gevorgyan, S. A.; Krebs, F. C. *Macromolecules* **2008**, *41*, 8986. (c) Helgesen, M.; Krebs, F. C. *Macromolecules* **2010**, *43*, 1253.

(17) Mak, C. S. K.; Leung, Q. Y.; Chan, W. K.; Djurišić, A. B. *Nanotechnology* **2008**, *19*, 424008.

(18) Beaupre, S.; Breton, A.; Dumas, J.; Leclerc, M. *Chem. Mater.* **2009**, *21*, 1504.

(19) Janietz, S.; Krueger, H.; Schleiermacher, H.; Wurfel, U.; Niggemann, M. *Macromol. Chem. Phys.* **2009**, *210*, 1493.

(20) Yen, W.; Pal, B.; Yang, J.; Hung, Y.; Lin, S.; Chao, C.; Su, W. *J. Polym. Sci., Part A: Polym. Chem.* **2009**, *47*, 5044.

(21) Mohamad, D.; Johnson, R. G.; Janeliunas, D.; Kirkus, M.; Yi, H.; Lidzey, D. G.; Iraqi, A. *J. Mater. Chem.* **2010**, *20*, 6990.

(22) Lai, M.; Tsai, J.; Chueh, C.; Wang, C.; Chen, W. *Macromol. Chem. Phys.* **2010**, *211*, 2017.

(23) Mak, C. S. K.; Cheung, W. K.; Leung, Q. Y.; Chan, W. K. *Macromol. Rapid Commun.* **2010**, *31*, 875.

(24) (a) Sonmez, G.; Shen, C. K. F.; Rubin, Y.; Wudl, F. *Angew. Chem., Int. Ed.* **2004**, *43*, 1948. (b) Sonmez, G.; Sonmez, H. B.; Shen, C. K. F.; Wudl, F. *Adv. Mater.* **2004**, *16*, 1905. (c) Sonmez, G.; Sonmez, H. B.; Shen, C. K. F.; Jost, R. W.; Rubin, Y.; Wudl, F. *Macromolecules* **2005**, *38*, 669.

(25) Tarkuc, S.; Unver, E. K.; Udum, Y. A.; Tanyeli, C.; Toppare, L. *Electrochim. Acta* **2010**, *55*, 7254.

(26) Wen, L.; Nietfeld, J. P.; Amb, C. M.; Rasmussen, S. C. *J. Org. Chem.* **2008**, *73*, 8529.

(27) Mulholland, M. E.; Schwiderski, R. L.; Rasmussen, S. C. *Polym. Bull.* **2012**, *69*, 291.

(28) Sforza, S.; Dossena, A.; Corradini, R.; Virgili, E.; Marchelli, R. *Tetrahedron Lett.* **1998**, *39*, 711.

(29) Baraznenok, I. L.; Nenajdenko, V. G.; Balenkova, E. S. *Tetrahedron* **2000**, *56*, 3077.

(30) Charette, A. B.; Grenon, M. *Can. J. Chem.* **2001**, *79*, 1694.

(31) Ghandi, M.; Salahi, S.; Hasani, M. *Tetrahedron Lett.* **2011**, *52*, 270.

(32) Sigel, H.; Martin, R. B. *Chem. Rev.* **1982**, *82*, 385.

(33) Fairlie, D. P.; Woon, T. C.; Wickramasinghe, W. A.; Willis, A. C. *Inorg. Chem.* **1994**, *33*, 6425.

(34) Kheifets, G. M.; Kol'stov, A. I.; Khachaturov, A. S.; Gindin, V. A. *Russ. J. Org. Chem.* **2000**, *36*, 1373.

(35) *CRC Handbook of Chemistry and Physics*; Weast, R. C, Ed.; CRC Press: Boca Raton, FL, 1987; p F-160.

(36) Van Bolhuis, F.; Wynberg, H. *Synth. Met.* **1989**, *30*, 381.

(37) *CRC Handbook of Chemistry and Physics*; Lide, D. R., Frederikse, H. P. R., Eds.; CRC Press: Boca Raton, FL, 1995; pp 9–6.

(38) Katritzky, A. R.; Pozharskii, A. F. *Handbook of Heterocyclic Chemistry*, 2nd ed.; Pergamon Press: New York, 2000; p 61.

(39) Antolini, L.; Horowitz, G.; Kouki, F.; Garnier, F. *Adv. Mater.* **1998**, *10*, 382.

(40) Herrema, J. K.; Wildeman, J.; van Bolhuis, F.; Hadziioannou, G. *Synth. Met.* **1993**, *60*, 239.

(41) Evenson, S. J.; Pappenfus, T. M.; Delgado, M. C. R.; Radke-Wohlers, K. R.; Navarrete, J. T. L.; Rasmussen, S. C. *Phys. Chem. Chem. Phys.* **2012**, *14*, 6101.

(42) Rasmussen, S. C.; Sattler, D. J.; Mitchell, K. A.; Maxwell, J. *J. Lumin.* **2004**, *190*, 111.

(43) Mo, H.; Radke, K. R.; Ogawa, K.; Heth, C. L.; Erpelding, B. T.; Rasmussen, S. C. *Phys. Chem. Chem. Phys.* **2010**, *12*, 14585.

(44) Turro, N. J. *Modern Molecular Photochemistry*; University Science Books: Sausalito, CA, 1991; p 106.

(45) Kenning, D. D.; Mitchell, K. A.; Calhoun, T. R.; Funfar, M. R.; Sattler, D. J.; Rasmussen, S. C. *J. Org. Chem.* **2002**, *67*, 9073.

(46) Heth, C. L.; Tallman, D. E.; Rasmussen, S. C. *J. Phys. Chem. B* **2010**, *114*, 5275.

(47) Meerholz, K.; Heinze, J. *Electrochim. Acta* **1996**, *41*, 1839.

(48) Ramkumar, D.; Kalpana, M.; Varghese, B.; Sankararaman, S. *J. Org. Chem.* **1996**, *61*, 2247.

(49) Zhou, Q.; Carroll, P. J.; Swager, T. M. *J. Org. Chem.* **1994**, *59*, 1294.

(50) Bradshaw, J. D.; Solooki, D.; Tessier, C. A.; Youngs, Y. J. *J. Am. Chem. Soc.* **1994**, *116*, 3177.

(51) (a) Waltman, R. J.; Diaz, A. F.; Bargon, J. *J. Electrochem. Soc.* **1984**, *131*, 1452. (b) Waltman, R. J.; Bargon, J. *Can. J. Chem.* **1986**, *64*, 76.

(52) Demanze, F.; Yassar, A.; Garnier, F. *Macromolecules* **1996**, *29*, 4267.
(53) Zuman, P. *Substituent Effects in Organic Polarography*; Plenum Press: New York, 1967.
(54) Pinhey, J. T.; Roche, E. G. *J. Chem. Soc., Perkins Trans. 1* **1988**, 2415.
(55) Kaslow, C. E.; Marsh, M. M. *J. Org. Chem.* **1947**, *12*, 456.
(56) Turro, N. J. *Modern Molecular Photochemistry*; University Science Books: Sausalito, CA, 1991; pp 86−90.
(57) Larson, R. C.; Iwamoto, R. T.; Adams, R. N. *Anal. Chim. Acta* **1961**, *25*, 371.